



Two-stage integrated process for bio-methanol production coupled with methane and carbon dioxide sequestration: Kinetic modelling and experimental validation

Krishna Kalyani Sahoo ^{a,1}, Swagata Datta ^{a,1}, Gargi Goswami ^b, Debasish Das ^{a,*}

^a Department of Biosciences & Bioengineering, Indian Institute of Technology, Guwahati, Assam, 781039, India

^b Department of Biotechnology, Gandhi Institute of Technology and Management (GITAM) University, Visakhapatnam, Andhra Pradesh, 530045, India

ARTICLE INFO

Keywords:

Methanotrophs
Bio-methanol
Methane
Carbon dioxide
Kinetic model

ABSTRACT

The study demonstrates a two-stage integrated process for bio-methanol production using *Methylosinus trichosporium* NCIMB 11131, coupled with sequestration of methane and carbon dioxide. The first stage involved generation of methanotropic biomass via sequestration of methane; which was used as biocatalyst to reduce carbon dioxide into methanol in the second stage. Maximum biomass titer of 3.39 g L^{-1} and productivity of $0.60 \text{ g L}^{-1} \text{ d}^{-1}$ were achieved in semi-batch stirred tank reactor with methane concentration in the inlet gas mixture of 2.5% v/v and gas flow rate of 0.5 vvm. Methane fixation rate was estimated to be $0.32 \text{ g L}^{-1} \text{ d}^{-1}$. Maximum methanol titer of 0.58 g L^{-1} was achieved at headspace carbon dioxide concentration of 50% v/v and liquid to headspace volume ratio 10:90. Subsequently, a kinetic model was developed to predict and understand the system behaviour in terms of dynamic profile of growth, methanol formation, concentration of dissolved methane or carbon dioxide in the aqueous phase and headspace carbon dioxide concentration, in response to varying process parameters. The model can serve as a tool for estimation of process parameters and aid in overall production optimization.

1. Introduction

Overpopulation and economic development have led to increased greenhouse gas emissions since the beginning of the pre-industrial era, resulting in unprecedented levels of atmospheric methane (CH_4) and carbon dioxide (CO_2) concentrations. The consequent effect has been reflecting through global climate change and enhanced global warming since the mid-20th century. Worldwide anthropogenic emission of CO_2 has almost hit 43.1 billion tonnes (Global Carbon Project Budget, 2019). Methane has a global warming potential 28–36 times that of CO_2 over a 100-year-timescale (US EPA, 2020). Furthermore, the global emission of methane stands at 570 million tonnes, of which 342 million tonnes is accounted for by anthropogenic sources, while the residual 228 million tonnes originate from natural reserves (e.g., wetlands, sediments, oceans, termites, biodegradation of organic wastes by methanogens, etc.) (IEA, Methane Tracker, 2020). There are ongoing efforts to transform these greenhouse gases into various value-added chemicals such as formaldehyde, ethanol, methanol, acetic acid, and formic acid (Wang

et al., 2017). Methanol, a widely used industrial solvent, is also known to be the precursor for synthesizing other chemicals like formaldehyde, acetic acid, dimethyl ether, and methyl tert-butyl ether (MTBE) (Dalen et al., 2018). Methanol is being considered as a potential transportation fuel owing to its high specific energy ratio, high heat of vaporization, low combustion temperature, high flame speed and so on (Verhelst et al., 2019). Although CH_4 is also used as a fuel, methanol stands superior to CH_4 in several ways: (i) methanol is a liquid at STP, which facilitates easy and safe storage and transportation with minimum product loss; (ii) methanol possesses 488-times greater volumetric energy content ($15,871 \text{ MJ m}^{-3}$) as compared to CH_4 (32.50 MJ m^{-3}) (Verhelst et al., 2019).

Methanol can be produced through chemical or biological route. Chemical synthesis of methanol may be achieved either through catalytic oxidation of CH_4 or via catalytic hydrogenation of CO_2 . However, the conventionally used chemical routes for methanol production are constrained by the requirement of: (i) expensive catalysts e.g., $\text{CuO}/\text{ZnO}/\text{Al}_2\text{O}_3$, $\text{Fe}_2\text{O}_3(\text{MoO}_3)_3$, $\text{MoO}_3/\text{SiO}_2$, $\text{MoO}_3/\text{Ga}_2\text{O}_3$, $\text{V}_2\text{O}_5/\text{SiO}_2$, etc.

* Corresponding author. Department of Biosciences & Bioengineering, Indian Institute of Technology Guwahati, Guwahati, Assam, 781039, India.

E-mail address: debasishd@iitg.ac.in (D. Das).

¹ The authors have contributed equally.

(i) extreme process conditions e.g., high temperature ($\sim 650^{\circ}\text{C}$) and pressure ($\sim 5 \text{ MPa}$) (Han et al., 2016; Zain and Mohamed, 2018); and (ii) release of carbon monoxide as one of the toxic by-products (Kumar et al., 2014). Alternatively, methanol can be produced biologically with the application of methanotrophic microorganisms as biocatalyst. Authors have reported various methanotrophic strains e.g., *Methylosinus trichosporium*, *Methylosinus sporium*, *Methyloferula stellata*, *Methylomicrobium album*, *Methylocella tundrae*, *Methylocystis bryophila* (Xin et al., 2007; Mardina et al., 2016; Patel et al., 2016b; Patel et al., 2020a, b, c), etc. for methanol production using noxious C1-carbon compounds, like CH_4 and CO_2 . Biological methods are advantageous over chemical methods as they operate under mild process conditions, without using expensive chemical catalysts; have low energy requirement, and higher conversion efficiency, accompanied with greater stability and selectivity, and hence may offer better economic feasibility; and are eco-friendly.

Methanotrophs are Gram-negative proteobacteria that utilize methane as their sole source of carbon and energy for growth. Methane, bio-sequestered by methanotrophs, is catalytically oxidized into methanol by methane monooxygenase (MMO), an endogenous irreversible enzyme. The produced methanol is subsequently converted into formaldehyde, formate, and CO_2 via sequential oxidations catalysed by three reversible enzymes: methanol dehydrogenase (MDH), formaldehyde dehydrogenase and formate dehydrogenase, respectively (Sahoo et al., 2021). A part of the intermediately produced formaldehyde/formate assimilates into the biomass as a carbon source via RuMP or serine pathway. MMO is classified into two types: particulate MMO (integrated on the cell membrane), and soluble MMO (produced in the cytoplasm). Particulate MMO shows elevated expression at high copper to biomass ratios, while the expression of soluble MMO increases under low copper to biomass ratios and high titre of iron ions. Soluble MMO causes faster methane oxidation relative to particulate MMO, owing to the higher substrate specificity of soluble MMO for methane (Sahoo et al., 2021). Methanotrophs are broadly classified into three types on the basis of the type of MMO synthesized. Type I methanotrophs (e.g., species of *Methylosoma*, *Methylothermus*, *Methylosarcina*, *Methylosphaera*, *Methylhalobius*, *Methylomonas*, *Methylobacter*, *Methylomicrobium*, *Crenothrix* and *Clonothrix*) express particulate MMO; Type II methanotrophs (e.g., species of *Methylocapsa*, *Methylocella*, *Methylosinus* and *Methylocystis*) express both soluble and particulate MMO; and Type X methanotrophs (e.g., species of *Methylococcus* and *Methylocaldum*) express certain specific properties of both Type I and Type II methanotrophs (Sahoo et al., 2021). For utilizing C1-carbon sources, Type I and Type X methanotrophs use RuMP pathway, while Type II methanotrophs use serine pathway (Sahoo et al., 2021). Type X methanotrophs vary from Type I owing to minimal expression of ribulose-bisphosphate carboxylase (an enzyme of serine cycle), occurring in Calvin-Benson-Bassham pathway (Park and Kim, 2019).

There have been initiatives on methanol production via MMO (soluble and particulate) catalysed biological oxidation of methane (Mardina et al., 2016; Patel et al., 2016a, 2020a). However, MDH and other enzymes cause subsequent sequential oxidation of the produced methanol into intermediate metabolites and CO_2 , resulting in decreased extracellular methanol accumulation (Sheets et al., 2016). To that end, various MDH inhibitors (e.g., NaCl , NH_4Cl , phosphate, EDTA, and MgCl_2) are supplemented in the fermentation media to increase methanol production (Patel et al., 2016a; Sheets et al., 2016). Although, particulate MMOs are also involved in the methanol production metabolism, but they do not require any cofactors for their activity. On the other hand, soluble MMOs require natural co-factor (NADH) regeneration for their activity and increased methanol accumulation. However, the MDH inhibitor-induced inhibition of methanol oxidation result in NADH depletion (Sahoo et al., 2021). Therefore, formate is exogenously added as a source of NADH, which is necessary to maintain the activity of soluble MMO in presence of MDH inhibitors (during soluble MMO-catalysed methanol production) and improved methanol titer

(Sheets et al., 2016; Patel et al., 2020c). Even with all these initiatives, a lower methanol titer in the range of 0.16–0.4 g L^{-1} (Hwang et al., 2015; Patel et al., 2016a; Mardina et al., 2016) has been achieved under native conditions in batch mode. Moreover, methanol production through biological oxidation of methane is constrained by high cost of pure CH_4 as feed, low methanol titer associated with low solubility of CH_4 in liquid medium, low CH_4 utilization efficiency and consequent slow growth rate of methanotrophs, and so on. Authors have tried to overcome these limitations through the use of biogas as low-cost feedstock (Sheets et al., 2016; Patel et al., 2020b), immobilization of cells/biocatalyst (Patel et al., 2020a, 2020b), repeated-batch cultures for reusability of cells (Patel et al., 2020b, 2020c), co-culture of cells for improved biocatalytic activity (Patel et al., 2020a) and, addition of methane vector to improve solubility (Patel et al., 2020c). An alternative to the current approaches could be the utilization of CO_2 , the end-product in the methanotrophic metabolism, as feedstock for methanol production. CO_2 , when fed to the cells in excess concentration, shifts the equilibrium in the backward direction (Xin et al., 2007). Since the activity of MMO is irreversible, the process results in the accumulation of methanol as an extracellular end-product (Xin et al., 2007).

Microbial metabolism, a biological process, involves high degree of complexity and exhibits significant variability with changes in growth conditions and environmental perturbation. To that end, a mechanistic model in synergy with experimental observations, can serve as an effective tool towards understanding the metabolism of a biological system. Various kinetic models have been proposed to understand phenotypic response of different biological systems involving methanotrophs e.g., metabolic coupling between oxygenic photosynthesis and methane oxidation during co-cultivation of photoautotroph and methanotroph (Badr et al., 2019); effect of nitrogen and oxygen on production of polyhydroxybutyrate (PHB) using *Methylocystis parvus* OBBP and *Methylosinus trichosporium* OB3b (Rostkowski et al., 2013); methane oxidation by the methanotrophic bacterial community in paddy soil (Cai and Yan, 1999); and degradation of chlorinated organic compounds by mixed methanotrophic culture (Chang and Alvarez-Cohen, 1997). However, till date no model has been reported to describe growth of the methanotroph using methane and exploitation of methanotrophic biomass as biocatalyst for conversion of CO_2 to methanol.

In the present study, we report a sequential two-stage integrated process for bio-methanol production using *Methylosinus trichosporium* NCIMB 11131, coupled with sequestration of methane and carbon dioxide. While, the first stage of the process involves generation of methanotrophic biomass via sequestration of methane as the sole carbon source; the second stage deals with the application of this biomass as biocatalyst for the reduction of CO_2 into methanol. High biomass titer and improved methane sequestration were achieved via optimization of process parameters e.g., methane percentage in the inlet gas stream and flow rate of the gas mixture in a semi-batch stirred tank reactor. To achieve an improved methanol titer, optimization of CO_2 concentration in the headspace and liquid to headspace volume ratio was carried out in an air tight batch reactor. Finally, a kinetic model was developed, which can be an effective tool to understand various phenotypic responses of the organism in terms of growth, methane sequestration, and methanol formation under the influence of varying process parameters. As another key outcome, the model was able to predict the dynamic profile for concentration of dissolved CH_4 , concentration of dissolved CO_2 , and headspace concentration of CO_2 .

2. Materials and methods

2.1. Organism and inoculum preparation

Methylosinus trichosporium NCIMB 11131 was procured from National Collection of Industrial Food and Marine Bacteria, and was cultured on nitrate mineral salt (NMS) medium (Patel et al., 2016a)

containing (g L^{-1}): KNO_3 (1.0), $\text{MgSO}_4 \cdot 6\text{H}_2\text{O}$ (1.0), CaCl_2 (0.2), Fe-EDTA (0.0038), $\text{Na}_2\text{MoO}_4 \cdot 2\text{H}_2\text{O}$ (0.00026), $\text{Na}_2\text{HPO}_4 \cdot 12\text{H}_2\text{O}$ (0.716), and KH_2PO_4 (0.26). Trace metal solution (1 mL) containing (g L^{-1}): $\text{CuSO}_4 \cdot 5\text{H}_2\text{O}$ (0.2), $\text{FeSO}_4 \cdot 7\text{H}_2\text{O}$ (0.5), $\text{ZnSO}_4 \cdot 7\text{H}_2\text{O}$ (0.4), H_3BO_3 (0.015), $\text{CoCl}_2 \cdot 6\text{H}_2\text{O}$ (0.05), EDTA di-sodium salt (0.25), $\text{MnCl}_2 \cdot 4\text{H}_2\text{O}$ (0.02), and $\text{NiCl}_2 \cdot 6\text{H}_2\text{O}$ (0.01) was added to the media. The pH of the medium was adjusted to 6.8 using 1 M NaOH and 1 M H_2SO_4 . All the chemicals were of analytical grade and procured from Himedia. All the reagents were prepared in Milli-Q water (18 MΩ). Inoculum preparation was carried out by culturing the cells in 500 mL customized air-tight bottles containing 100 mL of NMS medium at 30 °C in a shaker incubator (ORBITEK, Scigenics Biotech) at 150 rpm with intermittent sparging of methane. The mid-log phase culture (10% v/v) with an optical density of 5 was used as inoculum for all experiments.

2.2. Generation of methanotrophic biomass coupled with CH_4 sequestration

2.2.1. Characterisation of the organism in air-tight batch reactor

In the first step, characterization of the organism in terms of growth and CH_4 utilization was carried out in customized air-tight batch reactors (Borosil reagent bottles fitted with Duran bromo-butyl rubber stoppers) of 250 mL capacity with a working volume of 32 mL of NMS medium, under different concentrations of CH_4 (5%, 10%, 15%, 20%, 40%, 60%, and 80% v/v) in the headspace mixed with air. The organism was grown at 30 °C in a shaker incubator (ORBITEK, Scigenics Biotech) at 150 rpm for 96 h. Sampling was carried out at an interval of 24 h to obtain the dynamic profiles for growth and CH_4 utilization from headspace.

2.2.2. Characterisation of the organism in semi-batch stirred tank reactor

In the next step, the characterization of the organism was carried out in a customized semi-batch stirred-tank reactor of 1 L capacity containing 800 mL NMS medium under varying concentrations of CH_4 mixed with air in the inlet gas stream (1%, 2.5%, and 5% v/v) and different inlet gas flow-rates (0.25, 0.5, and 0.75 vvm). The reactor was equipped with a ring sparger with uniform pore sizes for continuous sparging of a gas mixture of methane and air. To maintain the cultivation temperature at 30 °C and facilitate efficient mass transfer of the continuously inflowing gases, the reactor was placed in a water bath on a hot-plate magnetic stirrer (IKA C-MAG HS7) with constant stirring (motor speed: 2.0). The concentration of CH_4 and the flow rate of the inlet gas stream were maintained using rotameters. Sampling was carried out at an interval of 8 h to obtain the dynamic profiles for growth. Methane fixation rate was calculated as per Eq. (1)

$$\text{Methane fixation rate } (\text{g L}^{-1} \text{d}^{-1}) = P_x \times E_c \times \left(\frac{16}{12} \right) \quad (1)$$

where, P_x is the biomass productivity ($\text{g L}^{-1} \text{d}^{-1}$), E_c is the elemental carbon content in the biomass. 16 and 12 are molecular weight of methane and carbon, respectively.

2.3. Methanol production

2.3.1. Methanotrophic biomass as biocatalyst for methanol production under different process conditions

The methanotrophic biomass, generated from the first stage, was evaluated for its potential to be used as a biocatalyst for methanol production from CO_2 under three different conditions: (i) the biomass was harvested from the first stage of growth and subsequently resuspended in freshly prepared NMS medium for methanol production in the second stage; (ii) a two-phase fermentation in NMS medium where, in the first phase, the organism was grown with CH_4 as the only carbon source followed by methanol production in the second phase utilizing CO_2 as the sole carbon source; & (iii) the biomass was harvested from the

first stage of growth and subsequently resuspended in 20 mM phosphate buffer medium containing 5 mM MgCl_2 (pH 6.8) for methanol production in the second stage, as per Xin et al. (2007). In all the three processes, methanol production experiments (second stage in case of processes i and iii or second phase in case of process ii) were carried out in customized air-tight batch reactors (Borosil reagent bottles fitted with Duran bromo-butyl rubber stoppers) of 250 mL capacity with a working volume of 40 mL of NMS medium or buffer solution, with a mixture of CO_2 and air (1:1 v/v) in the headspace. The cultures were incubated at 30 °C and 150 rpm. Sampling was carried out at regular time intervals to obtain dynamic profiles for methanol production and growth.

2.3.2. Effect of headspace CO_2 concentration and liquid to headspace volume ratio on methanol production

The effect of CO_2 composition and headspace volume on methanol production was studied in air-tight batch reactors (as described in section 2.2.1) as per Patel et al. (2016a, b) with minor modifications. The characterization was carried out in 20 mM phosphate buffer (pH 6.8) containing 5 mM MgCl_2 , using harvested biomass as biocatalyst (3.39 g L^{-1}). The culture was assessed for methanol production at varying CO_2 concentrations (10%, 30%, 40%, 50%, 60%, and 70% v/v) in the headspace with liquid to headspace volume ratio of 10:90. In the next step, the methanol production was evaluated under different liquid to headspace volume ratios (50:50, 40:60, 30:70, 20:80, and 10:90) maintaining optimal headspace CO_2 concentration at 50%. The cultures were incubated at 30 °C and 150 rpm. Sampling was carried out at regular time intervals to obtain dynamic profiles for methanol production and growth.

2.4. Analytical methods

To monitor cell growth, absorbance of the culture was measured at 600 nm (A_{600}) using UV-Vis spectrophotometer (Cary Series 100, Agilent Technologies). The absorbance values were converted into dry cell weight (DCW) using the correlation, one optical density = 0.42 g dry cells L^{-1} ($R^2 = 0.99$). Cell-free supernatant, obtained from centrifugation of the sample at 10,000 rpm for 15 min, was analysed for methanol formation. Methanol concentration in the sample was estimated by using high performance liquid chromatography (HPLC) (Ultimate 3000, Dionex, Thermo Fisher Scientific, Germany), as described previously (Mukherjee et al., 2019) for analysis of alcoholic solvents. Analysis of CH_4 concentration in the headspace of airtight batch reactor was carried out using gas chromatography (GC) (TRACE 1110, Thermo Scientific) equipped with Packed column (Restek PC2 6952, 15' x 1/8", mesh 80/100) and thermal conductivity detector (TCD). Argon was used as the carrier gas at a flow rate of 12 mL min^{-1} . The oven, injector, and detector temperatures were maintained at 40 °C, 150 °C, and 150 °C, respectively. Elemental composition (C, H, and N) of the biomass was carried out using CHNS analyser (EuroEA Elemental Analyser).

2.5. Model development

In the present study, a sequential two-stage process has been demonstrated, wherein the first stage is attributed to the generation of methanotrophic biomass by the utilization of CH_4 as the sole carbon source whereas, the second stage involves utilization of this biomass as biocatalyst towards the synthesis of methanol using CO_2 as the sole carbon source. The model was developed in the form of an unstructured kinetic model with the aim of capturing the phenotypic response of the organism such as growth, substrate utilization, and product formation under the influence of varying process parameters. In the first stage, the specific rate of growth, μ (Eq. (2)) of the organism was modelled in the form of modified Monod kinetics with methane dissolved in water (CH_4_L) as the limiting substrate. The mass balance equation for biomass (x) and dissolved methane are given by Eq. (3) and Eq. (4), respectively. In the second stage, the rate of production of methanol (P) was modelled

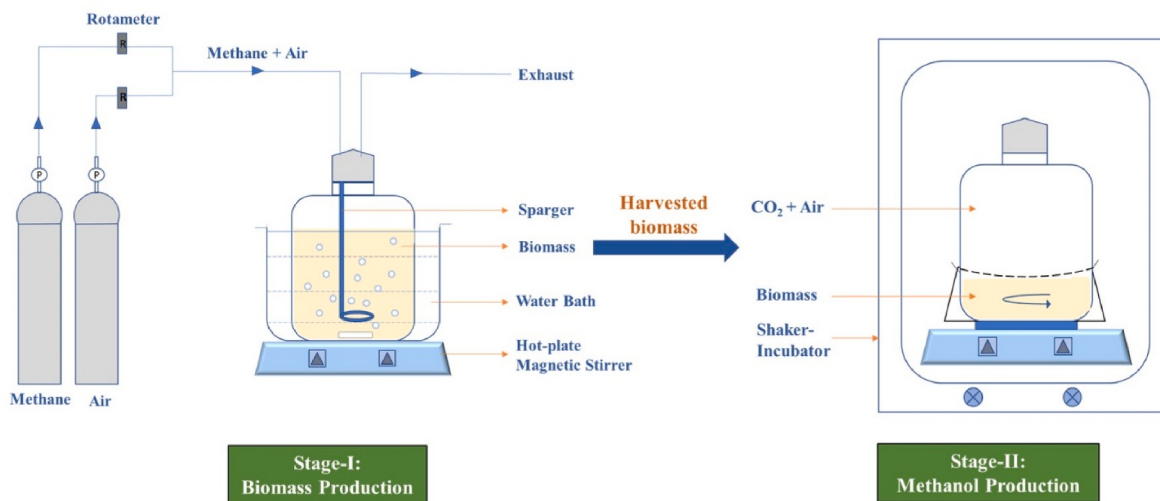


Fig. 1. Sequential two-stage integrated process for bio-methanol production.

in the form of Hill equation (Eq. (5)). The mass balance for dissolved carbon dioxide (CO_{2L}) and carbon dioxide concentration in the headspace (CO_{2G}) are given by Eq. (6) and Eq. (7), respectively. The solution for the model equation was obtained by solving the differential equations for growth and substrate utilization using non-stiff differential equation solver ‘ode 45’ available in the software package of MATLAB developed by MathWorks (Natick, MA).

Model Equations:

$$\mu = \left(\frac{\mu_{\max} \times (CH_4L)^n}{K_S + (CH_4L)^n} \right) \quad (2)$$

where, μ_{\max} is the maximum specific growth rate (h^{-1}) and K_S is the half saturation constant ($g L^{-1}$)

$$\frac{dx}{dt} = A \times \left(\frac{\mu_{\max} \times (CH_4L)^n \times x}{K_S + (CH_4L)^n} \right) \times \left(\frac{x_m - x}{x_m} \right) \quad (3)$$

where, x_m is the maximum biomass concentration ($g L^{-1}$)

$$\frac{dCH_4L}{dt} = k_{L,a_{CH_4}} \times \left(\frac{CH_4G}{H_{CH_4} \times R \times T} - CH_4L \right) - \left(\frac{1}{Y_{x/s}} \times \frac{dx}{dt} \right) \quad (4)$$

where, $k_{L,a_{CH_4}}$ is the volumetric mass transfer coefficient of CH_4 (h^{-1}); H_{CH_4} is the Henry’s constant for methane ($mol L^{-1} atm^{-1}$) and $Y_{x/s}$ is the biomass yield coefficient (g of biomass. g of substrate $^{-1}$).

$$\frac{dP}{dt} = Qp_{max} \times \left(\frac{A' \times (CO_{2L})^{n'}}{B + (CO_{2L})^{n'}} \right) \quad (5)$$

where, Qp_{max} is the maximum specific product formation rate (h^{-1})

$$\frac{dCO_{2L}}{dt} = k_{L,a_{CO_2}} \times \left(\frac{CO_{2G}}{H_{CO_2} \times R \times T} - CO_{2L} \right) - \left(\frac{1}{Y_{p/s}} \times \frac{dP}{dt} \right) \quad (6)$$

where, $k_{L,a_{CO_2}}$ is the volumetric mass transfer coefficient of CO_2 (h^{-1}); H_{CO_2} is the Henry’s constant for CO_2 ($mol L^{-1} atm^{-1}$) and $Y_{p/s}$ is the product yield coefficient (g of product. g of substrate $^{-1}$).

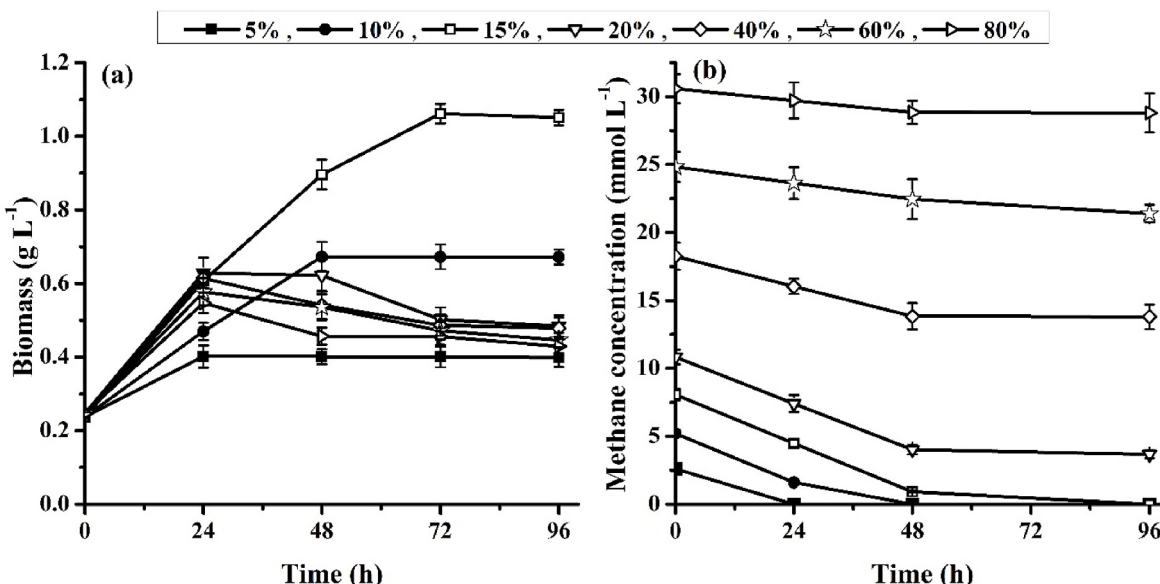


Fig. 2. Dynamic profile of (a) biomass and (b) methane concentration in the headspace. The organism was grown under different headspace gas compositions by varying the methane concentration from 5% to 80% v/v in an air-tight batch reactor.

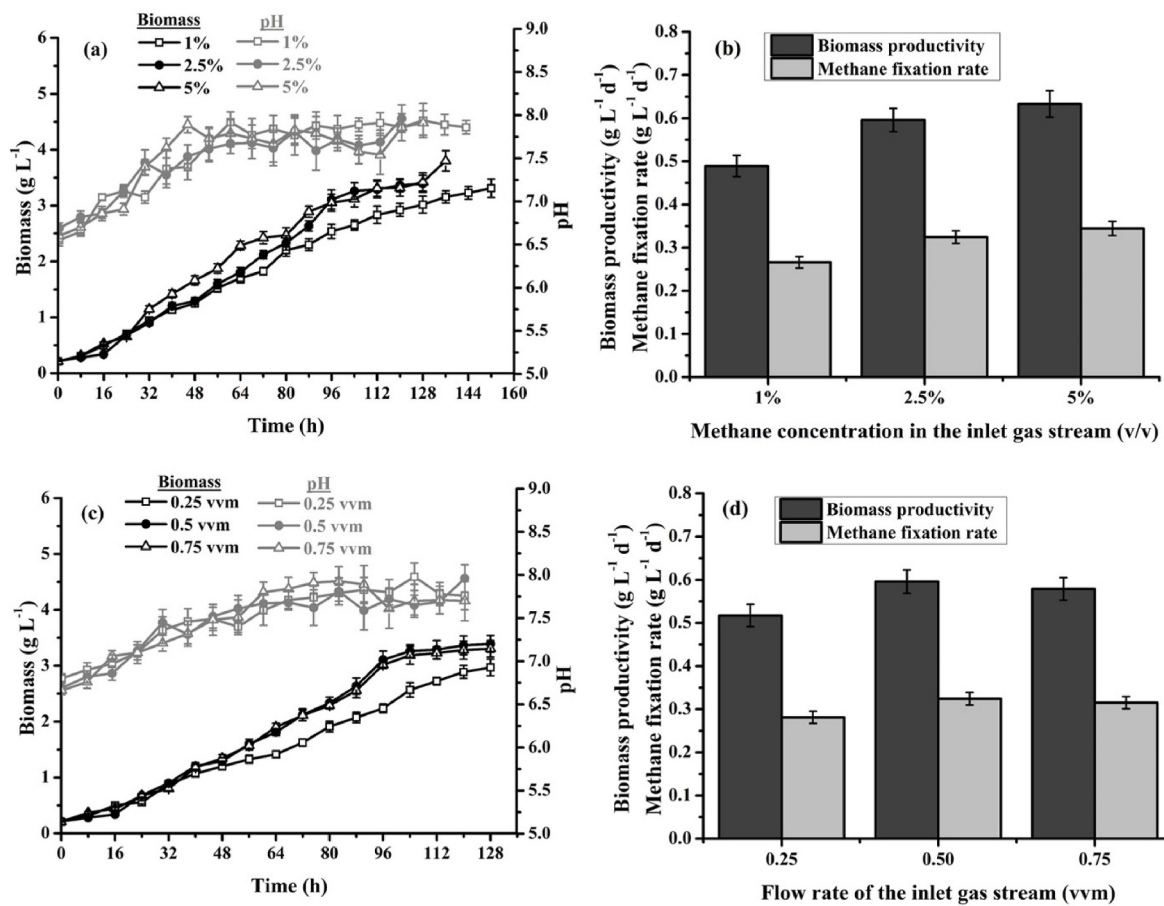


Fig. 3. Biomass titer (a & c) and pH (a & c), biomass productivity (b & d) and methane fixation rate (b & d) of *Methylosinus trichosporium* NCIMB 11131. The organism was grown under different methane concentrations in the inlet gas stream and flow rates of the inlet gas stream in a semi-batch stirred tank reactor.

$$\frac{d\text{CO}_2\text{G}}{dt} = - \left(k_L a_{\text{CO}_2} \cdot \left(\frac{\text{CO}_2\text{G}}{\text{H}_{\text{CO}_2} \times R \times T} - \text{CO}_2\text{L} \right) \right) \quad (7)$$

where, R is the universal gas constant ($0.0821 \text{ L-atm mol}^{-1} \text{ K}^{-1}$) and T is the cultivation temperature (K).

The experimental data obtained from various batch runs, as given in the previous sections, was used to estimate different model parameters such as stoichiometric coefficients and kinetic parameters, as well as for model validation for both the first and second stages of the process. The kinetic parameter values were estimated by fitting the simulated profile of the biomass and methanol formation with their corresponding experimental profiles. The values of the parameters which gave minimum deviation between simulated and experimental profile (goodness of fit was measured with the help of the R^2 value) were considered as the best estimate.

3. Results and discussion

In the sequential two-stage integrated process for bio-methanol production (Fig. 1), while the first stage involved generation of methanotrophic biomass via sequestration of methane as the sole carbon source; CO_2 was reduced to methanol in the second stage through the application of the methanotrophic biomass as biocatalyst.

3.1. First stage of methanotrophic biomass production with concomitant CH_4 sequestration

3.1.1. Growth of *M. trichosporium* in air-tight batch reactor

The extent of growth is the critical component that determined the

overall performance of the organism in terms of CH_4 sequestration and methanotrophic biomass generation. Therefore, it was essential to characterize the growth kinetics of *M. trichosporium* under various process parameters and modes of operation of the reactor. To that end, the organism was characterized for growth under different headspace gas compositions by varying the methane concentration from 5% to 80% v/v in an air-tight reactor operated under batch mode. Biomass titer was found to increase linearly with the increase in methane concentration from 5% and reached a maximum value of 1.06 g L^{-1} at a methane concentration of 15% (Fig. 2a). The maximum biomass productivity at 15% v/v CH_4 concentration was calculated to be $0.29 \text{ g L}^{-1} \text{ d}^{-1}$. Further increase in methane concentration beyond 15% resulted in significant reduction in growth of the organism. Low biomass titer at 5% (0.4 g L^{-1}) and 10% (0.67 g L^{-1}) methane concentrations may be attributed to the substrate limitation, as is evident from the complete utilization of methane from headspace within 48 h of cultivation (Fig. 2b). However, a reduction in biomass titer at higher methane concentrations of 20–80% may be attributed to the combinatorial effect of inadequate availability of methane in the liquid phase due to poor mass transfer and decreased concentration of oxygen in the reactor causing interference in the aerobic metabolism of the organism.

3.1.2. Growth of *M. trichosporium* in semi-batch stirred tank reactor

To overcome the key challenges of poor mass transfer of methane and substrate limitation, the growth of the organism was evaluated under continuous sparging of methane and air mixture in a semi-batch stirred tank reactor. At methane concentrations of 1%, 2.5%, and 5% v/v in the inlet gas stream with a flow rate of 0.5 vvm, the biomass titer was found to be comparable at 3.31 g L^{-1} , 3.39 g L^{-1} , and 3.8 g L^{-1} ,

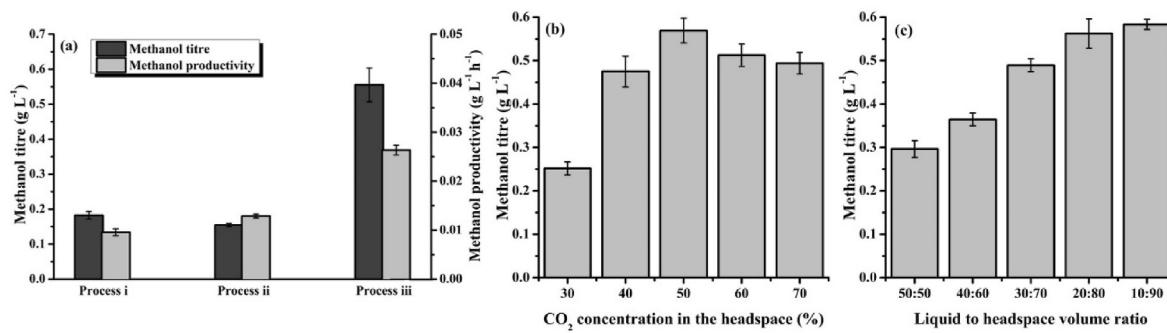


Fig. 4. (a) Methanol titer and productivity under three different process conditions; (b) methanol titer under varying concentration of CO₂ in the headspace and (c) methanol titer under different liquid to headspace volume ratios. The organism was grown in airtight batch reactor.

respectively (Fig. 3a). Further, the biomass productivity in the semi-batch mode was estimated to be in the range of 0.49 g L⁻¹ d⁻¹ – 0.63 g L⁻¹ d⁻¹ (Fig. 3b). The methane fixation rate was estimated to be comparable for growth at 2.5% (0.32 g L⁻¹ d⁻¹) and 5% (0.34 g L⁻¹ d⁻¹) methane concentration, respectively, albeit a marginally lower value was estimated for 1% methane concentration (0.27 g L⁻¹ d⁻¹) (Fig. 3b). Even though, the results indicate similar growth performance and methane fixation rate at 2.5% and 5% methane concentration in the inlet gas stream, the latter resulted in higher amount of unutilized methane being released into the atmosphere. Hence, subsequent experiments under different inlet gas flow rates were carried out with a methane concentration of 2.5%. While, at inlet gas flow rate of 0.25 vvm, biomass titer (2.97 g L⁻¹) and productivity (0.52 g L⁻¹ d⁻¹) was compromised marginally, these parameters remained comparable for both 0.5 vvm and 0.75 vvm (Fig. 3c and d). A similar profile was observed for methane fixation rate with values of 0.28 g L⁻¹ d⁻¹, 0.32 g L⁻¹ d⁻¹, and 0.32 g L⁻¹ d⁻¹ at inlet gas flow rates of 0.25, 0.5, and 0.75 vvm, respectively (Fig. 3d). The semi-batch stirred tank reactor with continuous gas sparging resulted in significant improvement in both biomass titer (~250%) and productivity (~120%) compared to the batch reactor. The semi-batch stirred tank reactor used in the present study enabled continuous supply of gas mixture using a sparger, located above the magnetic stirrer bar, resulting in uniform distribution of the gas bubbles. Constant mixing was achieved using magnetic stirrer, facilitating bottom-driven mass transfer. These attributes of the reactor prevented cell-settling and dead-zone formation thereby offering improved growth kinetics. The mass transfer of methane is the limiting step in the optimal performance of methanotrophic systems due to the low solubility of methane in aqueous solutions. Pauss et al. (1990) reported a three-fold increment in volumetric mass transfer coefficient ($k_L a$) value for CH₄ in a completely stirred tank reactor (0.09 h⁻¹) as compared to sludge bed reactor operated without mechanical stirring (0.03 h⁻¹). Therefore, in the present study, inlet methane concentration of 2.5% with a gas flow rate of 0.5 vvm was chosen for the generation of methanotrophic biomass in semi-batch stirred tank reactor resulting in biomass titer of 3.39 g L⁻¹ and productivity 0.60 g L⁻¹ d⁻¹.

Gilman et al. (2015) reported maximum biomass titer of 0.46 g L⁻¹ and average productivity of 0.23 g L⁻¹ d⁻¹ for continuous cultivation of *Methylomicrobium buryatense* with methane concentration of 2.5% mixed with air and fed at a flow rate of 100 mL min⁻¹. Cultivation of *M. trichosporium* OB3b in 5 L bioreactor with continuous flow of methane (140 mL min⁻¹) and air (1000 mL min⁻¹) for 240 h resulted in biomass titer of 2 g L⁻¹ (Han et al., 2009). Therefore, in the present study, biomass titer and productivity achieved for *Methylosinus trichosporium* NCIMB 11131 in semi-batch stirred tank reactor was found to be superior than the studies reported in the literature. The organism also exhibited improved performance in terms methane sequestration ability in comparison to the other methanotrophic fermentation processes. For instance, under chosen process parameters, both specific methane fixation rate of 45.44×10^{-4} g CH₄ g biomass⁻¹ h⁻¹ and volumetric

methane fixation rate of 0.32 g L⁻¹ d⁻¹ (0.84 mmol h⁻¹) were found to be higher than methanotrophic consortium (7.7×10^{-4} g CH₄ g biomass⁻¹ h⁻¹) grown in batch reactor containing 8% CH₄ (Cantera et al., 2016) and *Methylocaldum* sp. (0.54 mmol h⁻¹) in a trickle bed reactor (Sheets et al., 2017), respectively. However, higher volumetric methane fixation rate of ~0.98 g L⁻¹ d⁻¹ was reported for *Methylocystis hirsuta* grown in bubble column bioreactor coupled with internal gas re-circulation (Rodríguez et al., 2020).

Fig. 3a and c also present the profiles of pH during the growth of the organism. The pH was observed to vary within a range of 6.8–7.96. A pH range of 7–10 has been reported to be an optimum range for the growth of methanotrophs, via methane oxidation, without any adverse effect on their biocatalytic activity (Reddy et al., 2020).

3.2. Second stage for conversion of CO₂ into methanol using methanotrophic biomass

3.2.1. Evaluation of *M. trichosporium* as a potential biocatalyst for methanol biosynthesis under different process conditions

The highest methanol titer of 0.56 g L⁻¹ was recorded when the biomass was harvested from the first stage of growth and subsequently resuspended in phosphate buffer medium (Fig. 4a). However, methanol titer was found to reduce significantly (0.15–0.18 g L⁻¹) when either freshly prepared NMS medium or same NMS medium (used for the growth) was employed for methanol synthesis. Phosphate buffer also resulted in improved methanol productivity (0.026 g L⁻¹ h⁻¹) as compared to the other two process conditions (0.01–0.013 g L⁻¹ h⁻¹) (Fig. 4a). One of the key problems with methanol production from methane is the subsequent conversion of methanol into formaldehyde, catalysed by the enzyme methanol dehydrogenase (Sahoo et al., 2021). Several authors have reported the role of phosphate as an inhibitor for the enzyme methanol dehydrogenase, either by adding a specific concentration of phosphate to the NMS media (Han et al., 2013; Sheets et al., 2016) or by directly using phosphate buffer as a medium (Mardina et al., 2016; Patel et al., 2016a, 2020c) for methanol production via methane oxidation. Although in our study, methanol is being produced through the CO₂ reduction pathway, there may be a possibility of the back-conversion of methanol into intermediate metabolites and CO₂, owing to the reversible nature of the enzymes methanol dehydrogenase, formaldehyde dehydrogenase and formate dehydrogenase. This is where the role of phosphate buffer as a cultivation medium for methanol production from CO₂ comes into play, resulting in higher methanol titer and productivity relative to the NMS media. It is important to note that in none of the media, further growth of the organism was observed during methanol synthesis stage or phase (data not shown). In general, methanotrophic cells stay in the resting phase while being used as biocatalyst for methanol production from CO₂ (Xin et al., 2007) and hence do not require other media components to sustain their growth. Intracellularly stored NADH supply the reducing energy to accomplish the reduction of CO₂ to methanol. These reducing equivalents are produced

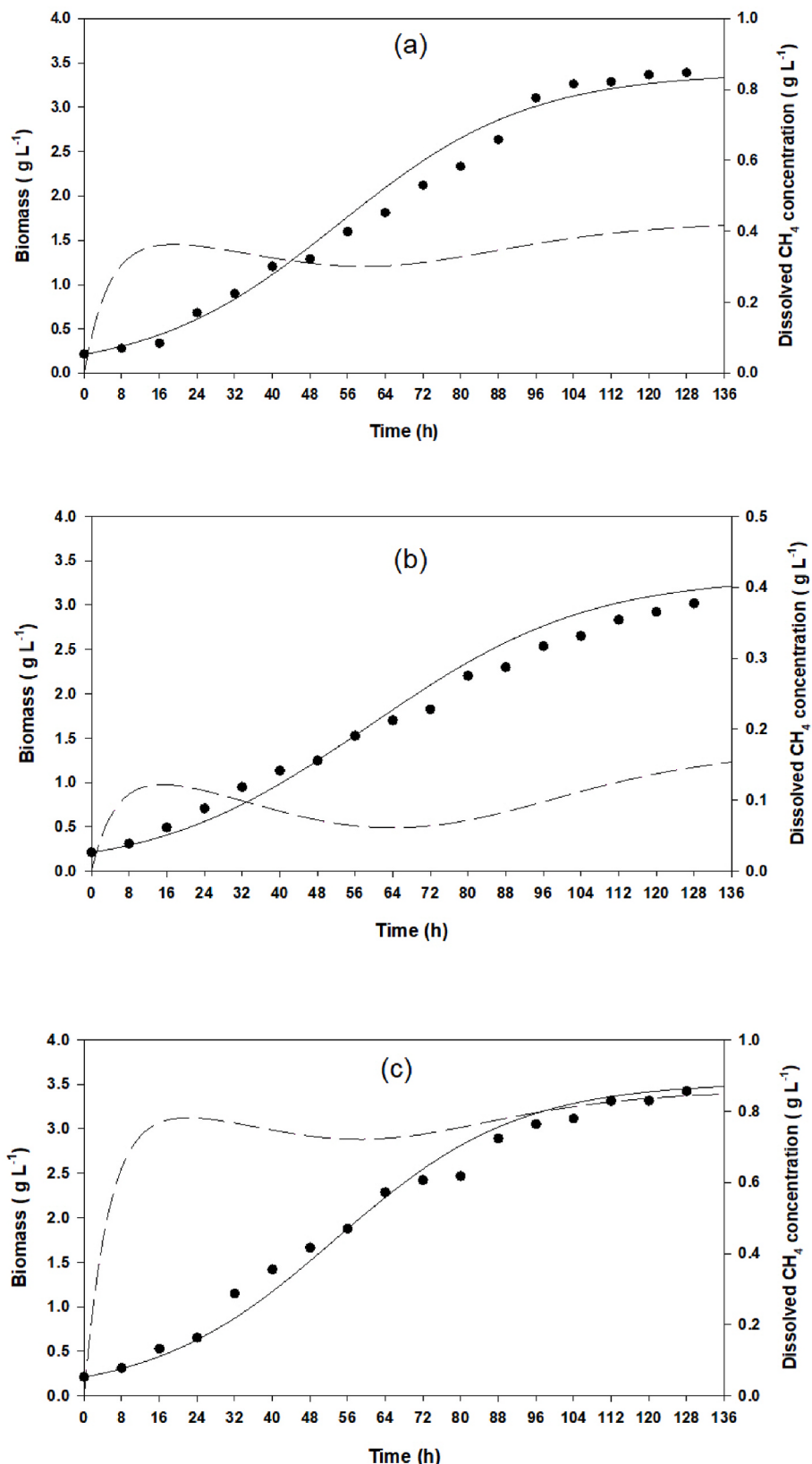


Fig. 5. Dynamic profile for growth and dissolved methane concentration at inlet methane concentration of (a) 2.5%, (b) 1% and (c) 5%. The symbol (●) represents experimental data for biomass and the lines represent simulated profiles for biomass (—) and dissolved methane concentration (—).

by the cell during the sequential oxidation of methane to CO₂ (first stage). In second stage, these reducing equivalents (in presence of excess CO₂) drive the equilibrium in backward direction causing the conversion of CO₂ into methanol (Xin et al., 2007). Therefore, phosphate buffer serves as the low-cost medium for methanol biosynthesis without any additional nutrient requirement.

3.2.2. Methanol production under varying CO₂ concentrations and liquid to headspace volume ratios

In the first step, methanol production was attempted in a semi-batch stirred tank reactor by continuous sparging of CO₂ (2.5% v/v) mixed with air at a flow rate of 0.5 vvm under atmospheric pressure. However, no methanol was detected in the extracellular medium. It has been reported that, at high partial pressure, the solubility of gases increases resulting in better interaction of the gaseous substrate with the key enzymes and in turn, positively regulates growth or product formation metabolism (Hurst and Lewis, 2010). Hence, in the present study, failure to induce methanol production in semi-batch stirred tank reactor may be attributed to the lower partial pressure of CO₂ in the gas mixture, which is considered to be the critical parameter for methanol production. Therefore, the second stage of methanol production was carried out in air-tight batch reactor with CO₂ mixed with air supplied in the headspace.

The extent of methanol formation was carried out under varying CO₂ concentrations in the headspace ranging from 10% to 70% v/v. No methanol was produced at the lowest CO₂ concentration of 10%. The methanol titer was found to increase concomitantly with the increase in CO₂ concentration from 30% and reached a maximum value of 0.57 g L⁻¹ (17.79 mM) at a CO₂ concentration of 50% (Fig. 4b). The CO₂ fixation percentage at 50% CO₂ concentration was estimated to be 8.95% of the initial amount of CO₂ present in the headspace. However, further increase in CO₂ concentration beyond 50% resulted in a marginal decrease in methanol titer. These results point towards the role of CO₂ partial pressure in the headspace as a critical parameter for methanol induction. However, down regulation of methanol biosynthesis at higher CO₂ partial pressure may be attributed to the possible inhibitory effect on enzymatic activity, electron transport chain, and carbon metabolism (Ceron-Chafla et al., 2020). There are a handful of studies towards the biological production of methanol via CO₂ reduction pathway. *Methylosinus sporium* was reported to produce methanol with a very low titer of 0.33 mM when grown in the presence of 30% CO₂ (Patel et al., 2016b). Xin et al. (2007) reported production of 0.004 μmol methanol per mg dry cell weight from *Methylosinus trichosporium* cells, using 55.5% CO₂ in the headspace. With the increase in liquid to headspace volume ratio from 50:50, methanol titer increased linearly and a maximum titer of 0.58 g L⁻¹ (18.10 mM) was obtained at a ratio of 10:90 (Fig. 4c). The corresponding CO₂ fixation percentage was estimated to be 9.06%. The results suggest that headspace volume is another process parameter influencing methanol production since it is directly linked to the availability of CO₂, as the substrate for reduction reaction, at a fixed partial pressure. Thus, the occurrence of the highest methanol titer at liquid to headspace volume ratio of 10:90 could be attributed to the absence of substrate limitation (Pen et al., 2014). Characterization of *M. sporium* towards methanol biosynthesis through methane oxidation under different headspace volumes resulted in highest titer of 5.40 mM at headspace volume of 83.33% (Patel et al., 2016a). Pen et al. (2014) reported an improved methanol titer of 290 mg L⁻¹ from methane biohydroxylation using *M. trichosporium* in batch reactor with 90% headspace volume as compared to cultivation with 37.5% headspace volume (35 mg L⁻¹). The biomass density remained almost constant during methanol production stage under varying CO₂ concentrations in the headspace and different liquid to headspace volume ratios (Fig. S1a, b; Supplementary material).

As discussed earlier, authors have reported several strategies to overcome the limitations associated with methanol production from biological oxidation of CH₄, including, use of biogas as feedstock, cell

Table 1

Model parameters for two-stage integrated process towards production of bio-methanol using methanotrophic biomass coupled with sequestration of methane and carbon dioxide.

Experimental condition	Model Parameters						
	Stage-I		Stage-II				
	μ_{\max} (h ⁻¹)	K _s (g L ⁻¹)	n	k _L aCH ₄ (h ⁻¹)	A	Y _{X/s} (g g ⁻¹)	x _m (g L ⁻¹)
2.5% CH ₄	0.07	0.07	0.5	0.19	0.8	1.72	3.39
1% CH ₄	0.07	0.07	0.5	0.19	0.8	1.7	3.31
5% CH ₄	0.07	0.07	0.5	0.19	0.8	1.72	3.52
Experimental condition							
Q _{p,max} (h ⁻¹)	A' (g L ⁻¹)	n'		k _L aCO ₂ (h ⁻¹)	B	Y _{p/s} (g g ⁻¹)	
50% CO ₂	0.02	5	1	0.11	0.02	0.68	
30% CO ₂	0.008	5	1	0.11	0.02	0.51	
70% CO ₂	0.018	5	1	0.11	0.02	0.43	

immobilization, repeated-batch cultivation, co-culture of cells, supplementation of methane vector, etc. (Sheets et al., 2016; Patel et al., 2020a, b, c). Despite of these approaches, the reported methanol titre is limited to the range of 5.37–13.42 mM (or, 0.17–0.43 g L⁻¹). Further, methanol production from biological reduction of CO₂, is also limited to a low methanol titer of up to 0.33 mM (Xin et al., 2007; Patel et al., 2016b). Therefore, it can be concluded that the maximum methanol titer achieved in the present study under optimum conditions is significantly higher than the similar studies reported in literature.

3.3. Model development for the sequential two-stage process

3.3.1. Kinetic modelling for the first stage

In the present study, batch data with inlet gas mixture composition of 2.5% CH₄ at 0.5 vvm flow-rate was used for the estimation of the model parameters (Fig. 5a). The model was subsequently validated with the experimental data from two batch runs with the inlet gas mixture composition of 1% (Fig. 5b) and 5% CH₄ (Fig. 5c) at a flow rate of 0.5 vvm.

Estimation of parameters in reaction kinetic expressions is an essential step during the development of a process model. In the present study, while the biomass yield coefficient (Y_{X/s}), maximum specific growth rate (μ_{\max}), and maximum biomass concentration (x_m) were derived from experimental data of various batch runs, the other kinetic parameters, such as half-saturation constant (K_s), volumetric mass transfer coefficient for methane (k_LaCH₄) and model constants such as, n and A were determined by parameter estimation (Table 1). The values of universal gas constant (R = 0.0821 L-atm mol⁻¹ K⁻¹) and Henry's constant for methane (H_{CH₄} = 0.0015 mol L⁻¹ atm⁻¹) were obtained from literature (Meylan and Howard, 1991; Lovley et al., 1994). In a fermentation process, when substrate concentration is higher than K_s, the specific growth rate of the bacteria is also higher, often approaching the maximum specific growth rate. When substrate concentration becomes equal to or less than K_s, the specific growth rate of the bacteria reduces, implying that there is an inherent substrate limitation in the system (Grady et al., 2011). According to the parameters estimated for the present model, the value of K_s (0.07 g L⁻¹) was found to be lower than the dissolved CH₄ concentration of approximately 0.35 g L⁻¹ (Fig. 5a) at any given point of time. This implies that there was negligible substrate limitation in the semi-batch system employed for the purpose of this study. Kovárová-Kovar and Egli (1998) interpreted 1/K_s as the affinity of a cell towards the substrate, where a lower K_s value corresponds to a higher substrate affinity. A low K_s value can also imply a higher conversion of substrate into biomass. This implication is in line with the affinity concept that associates low K_s value to larger harvest volumes (Ugalde-Salas et al., 2020). The k_La value for the semi-batch

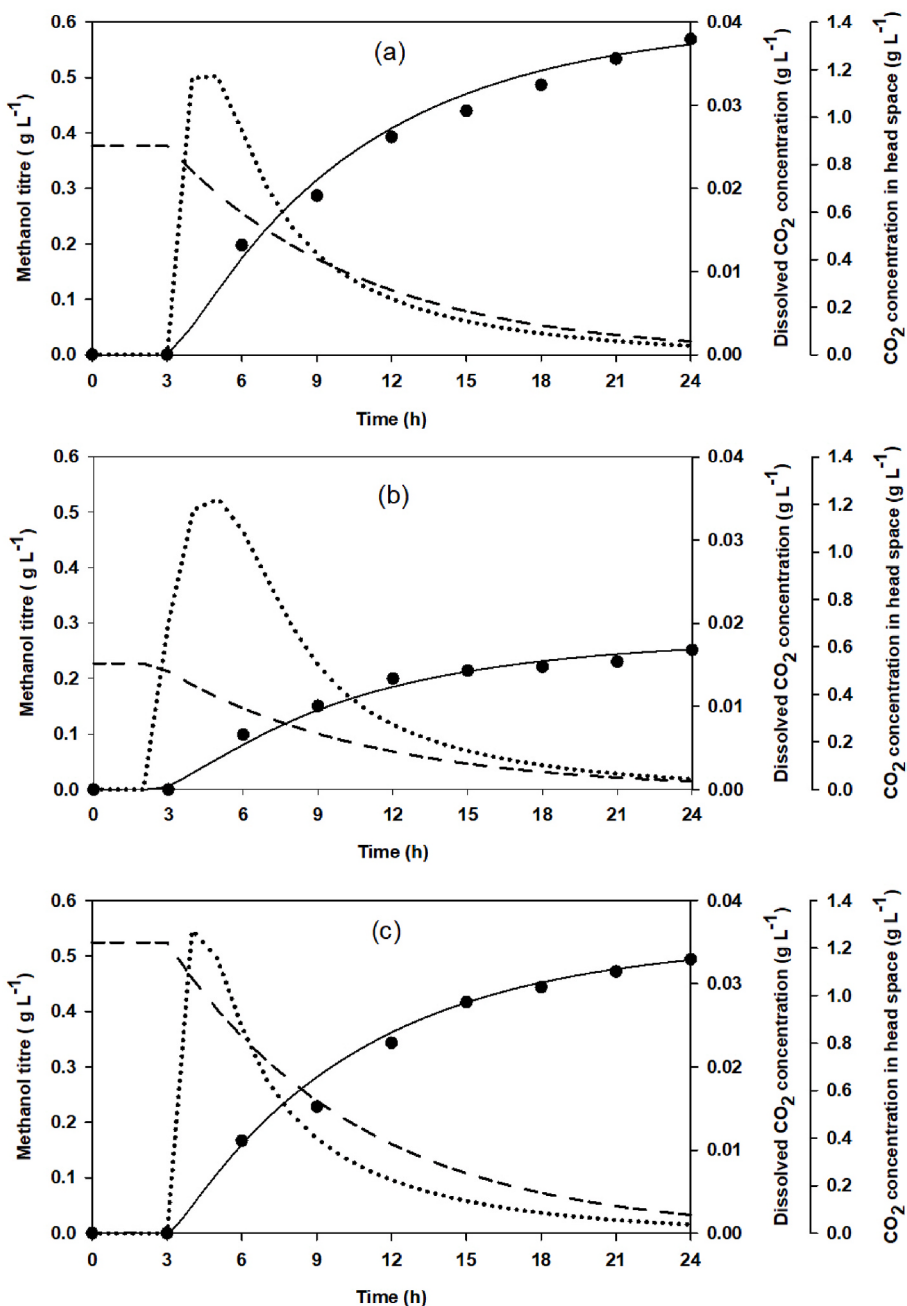


Fig. 6. Dynamic profile for methanol titer, dissolved CO₂ concentration and headspace CO₂ concentration, at varying CO₂ composition of (a) 50%, (b) 30% and (c) 70%. The symbol (●) represents experimental data for methanol titer and the lines represent simulated profiles for methanol titer (—), dissolved CO₂ concentration (....) and headspace CO₂ concentration (—).

reactor was estimated to be 0.19 h⁻¹. This value is in a feasible range, as inferred from the studies of Pauss et al. (1990) who previously reported a k_{L_a} value for methane of 0.09 h⁻¹ in a completely stirred tank reactor at steady state.

The model was able to predict the growth profiles of the organism at methane concentrations of 1% (Fig. 5b) and 5% (Fig. 5c) in the gas mixture accurately. Further, the model provided an insight into the dissolved methane concentration profile (Fig. 5) as one of the key outputs, thereby offering an easy alternate solution to energy intensive and expensive experimental methods (Aldhafeeri et al., 2020). As the gas was continuously sparged throughout the batch run, the overall methane concentration initially increased and reached a saturation value, beyond which it was approximately constant (Fig. 5). A decrease in the concentration of dissolved methane was observed from 21 h to

100 h, implying a higher substrate uptake rate due to the exponential growth phase of the bacteria.

3.3.2. Kinetic modelling for the second stage

For the second stage of the model, batch data with 50% CO₂ (Fig. 6a) in the headspace was used for the estimation of model parameters. The model was subsequently validated with the experimental data from two batch runs with headspace CO₂ concentration of 30% (Fig. 6b) and 70% (Fig. 6c). While specific product formation rate ($Q_{p_{max}}$) was derived from experimental data, the kinetic and stoichiometric parameters such as product yield coefficient ($Y_{p/s}$) and volumetric mass transfer coefficient for carbon dioxide ($k_{L_a CO_2}$) were estimated (Table 1). The value of Henry's constant for carbon dioxide ($H_{CO_2} = 0.033 \text{ mol L}^{-1} \text{ atm}^{-1}$) was obtained from literature (Sander et al., 2011). With the change in CO₂

concentration, $Q_{P\max}$ was found to vary within a narrow range of 0.008–0.02 h⁻¹. However, the product yield coefficient (Y_p/s, g of methanol per g of CO₂ consumed) was found to vary significantly within the range of 0.43–0.68. The value of $k_L a_{CO_2}$ was estimated to be 0.11 h⁻¹, comparable with that of methane.

In the second stage, the model predicted profiles of methanol formation was found to be in good agreement with the experimental data for both 30% (Fig. 6b) and 70% CO₂ (Fig. 6c) concentration in the headspace. An initial lag phase of approximately 3 h in methanol production was observed in all the three batch experiments. This lag phase may be attributed to the delayed induction in the mass transfer of CO₂ from headspace to the liquid phase (Fig. 6). Beyond the initial lag phase of 3 h, a gradual decrease in headspace CO₂ concentration was predicted till the end of the batch (Fig. 6). Post lag phase, an initial increase in dissolved CO₂ concentration was found to be concomitant with the decrease in headspace CO₂ concentration, after which the bacteria actively utilized it to produce methanol, leading to a significant decrease in dissolved CO₂ concentration beyond 5 h. The dissolved CO₂ concentration eventually became zero, at which point the methanol production was also seen to be saturated.

4. Conclusions

Two-stage integrated bioprocess was demonstrated for bio-methanol synthesis using *M. trichosporium* coupled with sequestration of methane and carbon dioxide. Improved biomass titer, methane fixation rate and methanol titer was achieved via optimization of process parameters. Semi-batch stirred tank reactor used in the first stage addresses the key challenge of mass transfer limitation of methane from gas to liquid phase. Methanol titer in the second stage was found to be critically dependent on the partial pressure of carbon dioxide in the headspace of batch reactor. A kinetic model was developed to capture phenotypic response of the methanotroph under varying process parameters.

Credit author statement

Krishna Kalyani Sahoo: Experimentation, analysis and interpretation of data, and manuscript preparation. **Swagata Datta:** Experimentation, development and validation of kinetic model, and manuscript preparation. **Gargi Goswami:** Conceptualization and manuscript writing. **Debasish Das:** Conceptualization, overall supervision of the work and manuscript writing.

Declaration of competing interest

The authors declare that they have no known competing financial interests or personal relationships that could have appeared to influence the work reported in this paper.

Acknowledgements

Krishna Kalyani Sahoo and Swagata Datta are grateful to Ministry of Education, Government of India for their research fellowships.

Appendix A. Supplementary data

Supplementary data to this article can be found online at <https://doi.org/10.1016/j.jenvman.2021.113927>.

References

- Aldhafeeri, T., Tran, M.K., Vrolyk, R., Pope, M., Fowler, M., 2020. A review of methane gas detection sensors: recent developments and future perspectives. Invent 5 (3), 28. <https://doi.org/10.3390/inventions5030028>.
- Badr, K., Hilliard, M., Roberts, N., He, Q.P., Wang, J., 2019. Photoautotrophic-methanotroph coculture—a flexible platform for efficient biological CO₂-CH₄ CO-utilization. IFAC-PapersOnLine 52 (1), 916–921. <https://doi.org/10.1016/j.ifacol.2019.06.179>.
- Cai, Z., Yan, X., 1999. Kinetic model for methane oxidation by paddy soil as affected by temperature, moisture and N addition. Soil Biol. Biochem. 31 (5), 715–725. [https://doi.org/10.1016/S0038-0717\(98\)00170-9](https://doi.org/10.1016/S0038-0717(98)00170-9).
- Cantera, S., Lebrero, R., García-Encina, P.A., Muñoz, R., 2016. Evaluation of the influence of methane and copper concentration and methane mass transport on the community structure and biodegradation kinetics of methanotrophic cultures. J. Environ. Manag. 171, 11–20. <https://doi.org/10.1016/j.jenvman.2016.02.002>.
- Ceron-Chafla, P., Kleerebezem, R., Rabaey, K., van Lier, J.B., Lindeboom, R.E., 2020. Direct and indirect effects of increased CO₂ partial pressure on the bioenergetics of syntrophic propionate and butyrate conversion. Environ. Sci. Technol. 54 (19), 12583–12592. <https://doi.org/10.1021/acs.est.0c02022>.
- Chang, H.L., Alvarez-Cohen, L., 1997. Two-stage methanotrophic bioreactor for the treatment of chlorinated organic wastewater. Water Res. 31 (8), 2026–2036. [https://doi.org/10.1016/S0043-1354\(97\)00020-1](https://doi.org/10.1016/S0043-1354(97)00020-1).
- Dalena, F., Senatore, A., Marino, A., Gordano, A., Basile, M., Basile, A., 2018. Methanol production and applications: an overview. Methanol 3–28. <https://doi.org/10.1016/B978-0-444-63903-5.00001-7>.
- Gilman, A., Laurens, L.M., Puri, A.W., Chu, F., Pienkos, P.T., Lidstrom, M.E., 2015. Bioreactor performance parameters for an industrially-promising methanotroph *Methylomicrobium buryatense* 5GB1. Microb. Cell Factories 14 (1), 1–8. <https://doi.org/10.1186/s12934-015-0372-8>.
- Global Carbon Budget, 2019. Global Carbon Project. <https://www.globalcarbonproject.org/carbonbudget/>. (Accessed 9 June 2021). accessed.
- Grady Jr., C.L., Daigger, G.T., Love, N.G., Filipe, C.D., 2011. Biological Wastewater Treatment. CRC press.
- Han, B., Su, T., Wu, H., Gou, Z., Xing, X.H., Jiang, H., Chen, Y., Li, X., Murrell, J.C., 2009. Paraffin oil as a “methane vector” for rapid and high cell density cultivation of *Methylosinus trichosporium* OB3b. Appl. Microbiol. Biotechnol. 83 (4), 669–677. <https://doi.org/10.1007/s00253-009-1866-2>.
- Han, B., Yang, Y., Xu, Y., Etim, U.J., Qiao, K., Xu, B., Yan, Z., 2016. A review of the direct oxidation of methane to methanol. Chin. J. Catal. 37 (8), 1206–1215. [https://doi.org/10.1016/S1872-2067\(15\)61097-X](https://doi.org/10.1016/S1872-2067(15)61097-X).
- Han, J.S., Ahn, C.M., Mahanty, B., Kim, C.G., 2013. Partial oxidative conversion of methane to methanol through selective inhibition of methanol dehydrogenase in methanotrophic consortium from landfill cover soil. Appl. Biochem. Biotechnol. 171 (6), 1487–1499. <https://doi.org/10.1007/s12010-013-0410-0>.
- Hurst, K.M., Lewis, R.S., 2010. Carbon monoxide partial pressure effects on the metabolic process of syngas fermentation. Biochem. Eng. J. 48 (2), 159–165. <https://doi.org/10.1016/j.bej.2009.09.004>.
- Hwang, I.Y., Hur, D.H., Lee, J.H., Park, C.H., Chang, I.S., Lee, J.W., Lee, E.Y., 2015. Batch conversion of methane to methanol using *Methylosinus trichosporum* OB3b as biocatalyst. J. Microbiol. Biotechnol. 25 (3), 375–380. <https://doi.org/10.4014/jmb.1412.12007>.
- Kovárová-Kovář, K., Egli, T., 1998. Growth kinetics of suspended microbial cells: from single-substrate-controlled growth to mixed-substrate kinetics. Microbiol. Mol. Biol. Rev. 62 (3), 646. <https://doi.org/10.1128/MMBR.62.3.646-666.1998>.
- Kumar, P., Kumar, A., Sreedhar, B., Sain, B., Ray, S.S., Jain, S.L., 2014. Cobalt phthalocyanine immobilized on graphene oxide: an efficient visible-active catalyst for the photoreduction of carbon dioxide. Chem. Eur. J. 20 (20), 6154–6161. <https://doi.org/10.7939/r3-cvhq-tm43>.
- Lovley, D.R., Chapelle, F.H., Woodward, J.C., 1994. Use of dissolved H₂ concentrations to determine distribution of microbially catalyzed redox reactions in anoxic groundwater. Environ. Sci. Technol. 28 (7), 1205–1210. <https://doi.org/10.1021/es00056a005>.
- Mardina, P., Li, J., Patel, S.K., Kim, I.W., Lee, J.K., Selvaraj, C., 2016. Potential of immobilized whole-cell *Methylocella tundrae* as a biocatalyst for methanol production from methane. J. Microbiol. Biotechnol. 26 (7), 1234–1241. <https://doi.org/10.4014/jmb.1602.02074>.
- Methane Tracker, 2020. International Energy Agency. <https://www.iea.org/reports/methane-tracker-2020>. (Accessed 9 August 2021). accessed.
- Meylan, W.M., Howard, P.H., 1991. Bond contribution method for estimating Henry's law constants. Environ. Toxicol. Chem.: Int. J. 10 (10), 1283–1293. <https://doi.org/10.1002/etc.5620101007>.
- Mukherjee, M., Sarkar, P., Goswami, G., Das, D., 2019. Regulation of butanol biosynthesis in *Clostridium acetobutylicum* ATCC 824 under the influence of zinc supplementation and magnesium starvation. Enzym. Microb. Technol. 129, 109352. <https://doi.org/10.1016/j.enzmictec.2019.05.009>.
- Park, S.Y., Kim, C.G., 2019. Application and development of methanotrophs in environmental engineering. J. Mater. Cycles Waste Manag. 21, 415–422. <https://doi.org/10.1007/s10163-018-00826-w>.
- Patel, S.K., Selvaraj, C., Mardina, P., Jeong, J.H., Kalia, V.C., Kang, Y.C., Lee, J.K., 2016a. Enhancement of methanol production from synthetic gas mixture by *Methylosinus spumtorum* through covalent immobilization. Appl. Energy 171, 383–391. <https://doi.org/10.1016/j.apenergy.2016.03.022>.
- Patel, S.K., Mardina, P., Kim, D., Kim, S.Y., Kalia, V.C., Kim, I.W., Lee, J.K., 2016b. Improvement in methanol production by regulating the composition of synthetic gas mixture and raw biogas. Bioresour. Technol. 218, 202–208. <https://doi.org/10.1016/j.biortech.2016.06.065>.
- Patel, S.K., Gupta, R.K., Kumar, V., Kondaveeti, S., Kumar, A., Das, D., Kalia, V.C., Lee, J. K., 2020a. Biomethanol production from methane by immobilized co-cultures of methanotrophs. Indian J. Microbiol. 60, 318–324. <https://doi.org/10.1007/s12088-020-00883-6>.
- Patel, S.K., Gupta, R.K., Kondaveeti, S., Otari, S.V., Kumar, A., Kalia, V.C., Lee, J.K., 2020b. Conversion of biogas to methanol by methanotrophs immobilized on

- chemically modified chitosan. *Bioresour. Technol.* 315, 123791. <https://doi.org/10.1016/j.biortech.2020.123791>.
- Patel, S.K., Shamugam, R., Kalia, V.C., Lee, J.K., 2020c. Methanol production by polymer-encapsulated methanotrophs from simulated biogas in the presence of methane vector. *Bioresour. Technol.* 304, 123022. <https://doi.org/10.1016/j.biortech.2020.123022>.
- Pauss, A., Andre, G., Perrier, M., Guiot, S.R., 1990. Liquid-to-gas mass transfer in anaerobic processes: inevitable transfer limitations of methane and hydrogen in the biomethanation process. *Appl. Environ. Microbiol.* 56 (6), 1636. <https://doi.org/10.1128/aem.56.6.1636-1644.1990>.
- Pen, N., Soussan, L., Belleville, M.P., Sanchez, J., Charmette, C., Paolucci-Jeanjean, D., 2014. An innovative membrane bioreactor for methane biohydroxylation. *Bioresour. Technol.* 174, 42–52. <https://doi.org/10.1016/j.biortech.2014.10.001>.
- Reddy, K.R., Rai, R.K., Green, S.J., Chettri, J.K., 2020. Effect of pH on methane oxidation and community composition in landfill cover soil. *J. Environ. Eng.* 146 (6), 04020037 [https://doi.org/10.1061/\(ASCE\)EE.1943-7870.0001712](https://doi.org/10.1061/(ASCE)EE.1943-7870.0001712).
- Rodríguez, Y., Firmino, P.I.M., Pérez, V., Lebrero, R., Muñoz, R., 2020. Biogas valorization via continuous polyhydroxybutyrate production by *Methylocystis hirsuta* in a bubble column bioreactor. *Waste Manag.* 113, 395–403. <https://doi.org/10.1016/j.wasman.2020.06.009>.
- Rostkowski, K.H., Pfluger, A.R., Criddle, C.S., 2013. Stoichiometry and kinetics of the PHB-producing Type II methanotrophs *Methylosinus trichosporium* OB3b and *Methylocystis parvus* OBBP. *Bioresour. Technol.* 132, 71–77. <https://doi.org/10.1016/j.biortech.2012.12.129>.
- Sahoo, K.K., Goswami, G., Das, D., 2021. Biotransformation of methane and carbon dioxide into high-value products by methanotrophs: current state of art and future prospects. *Front. Microbiol.* 12, 520. <https://doi.org/10.3389/fmicb.2021.636486>.
- Sander, S.P., Friedl, R.R., Barker, J.R., Golden, D.M., Kurylo, M.J., Wine, P.H., Abbatt, J.P.D., Burkholder, J.B., Kolb, C.E., Moortgat, G.K., Huie, R.E., 2011. Chemical Kinetics and Photochemical Data for Use in Atmospheric Studies, Evaluation Number 14, vol. 10. *JPL Publ.*
- Sheets, J.P., Ge, X., Li, Y.F., Yu, Z., Li, Y., 2016. Biological conversion of biogas to methanol using methanotrophs isolated from solid-state anaerobic digestate. *Bioresour. Technol.* 201, 50–57. <https://doi.org/10.1016/j.biortech.2015.11.035>.
- Sheets, J.P., Lawson, K., Ge, X., Wang, L., Yu, Z., Li, Y., 2017. Development and evaluation of a trickle bed bioreactor for enhanced mass transfer and methanol production from biogas. *Biochem. Eng. J.* 122, 103–114. <https://doi.org/10.1016/j.bej.2017.03.006>.
- Ugalde-Salas, P., Desmond-Le Quéméner, E., Harmand, J., Rapaport, A., Bouchez, T., 2020. Insights from microbial transition state theory on Monod's affinity constant. *Sci. Rep.* 10 (1), 1–4. <https://doi.org/10.1038/s41598-020-62213-6>.
- Understanding Global Warming Potentials, 2020. United States Environmental Protection Agency. <https://www.epa.gov/ghgemissions/understanding-global-warming-potentials>. (Accessed 9 August 2021). accessed.
- Verhelst, S., Turner, J.W., Sileghem, L., Vancoillie, J., 2019. Methanol as a fuel for internal combustion engines. *Prog. Energy Combust. Sci.* 70, 43–88. <https://doi.org/10.1016/j.pecs.2018.10.001>.
- Wang, L., Yi, Y., Wu, C., Guo, H., Tu, X., 2017. One-step reforming of CO₂ and CH₄ into high-value liquid chemicals and fuels at room temperature by plasma-driven catalysis. *Angew. Chem. Int. Ed.* 56 (44), 13679–13683. <https://doi.org/10.1002/anie.201707131>.
- Xin, J.Y., Zhang, Y.X., Zhang, S., Xia, C.G., Li, S.B., 2007. Methanol production from CO₂ by resting cells of the methanotrophic bacterium *Methylosinus trichosporium* IMV 3011. *J. Basic Microbiol.* 47 (5), 426–435. <https://doi.org/10.1002/jobm.200710313>.
- Zain, M.M., Mohamed, A.R., 2018. An overview on conversion technologies to produce value added products from CH₄ and CO₂ as major biogas constituents. *Renew. Sustain. Energy Rev.* 98, 56–63. <https://doi.org/10.1016/j.rser.2018.09.003>.